Mode interference and periodic self-focusing of spin waves in permalloy microstripes

Vladislav E. Demidov* and Sergej O. Demokritov
Institute for Applied Physics and Center for Nonlinear Science, University of Muenster, Corrensstrasse 2-4, 48149 Muenster, Germany

Karsten Rott, Patryk Krzysteczko, and Guenter Reiss
Department of Physics, Bielefeld University, P.O. Box 100131, 33501 Bielefeld, Germany
(Received 18 December 2007; published 4 February 2008)

We have studied propagation of spin waves in transversally magnetized permalloy microstripes. Our findings show that the interference of spin-wave modes quantized in the direction perpendicular to the stripe axis leads to a spatial pattern characterized by a periodic concentration of the spin-wave energy in the middle of the stripe, which can also be considered as a periodic self-focusing of spin waves. We present a simple model connecting the spatial period of the interference pattern with the width of the stripe and the spin-wave frequency. The studied phenomenon can be used for efficient transmission and processing of microwave-frequency signals by means of spin waves on the nanometer scale.

DOI: 10.1103/PhysRevB.77.064406 PACS number(s): 75.40.Gb, 75.30.Ds, 75.75.+a, 85.75.−d

Since the first observations of spin-wave quantization effects in magnetic microstripes,[1,2] the interest on the high-frequency magnetization dynamics in ferromagnetic film structures with submicrometer lateral dimensions has been growing continuously (see, e.g., Refs. 3–27). These investigations are important for a deep understanding of the basic physics of magnetic phenomena on the microscopic scale, as well as for technical applications of magnetic nanostructures for high-speed signal processing and information storage technologies. Recently, propagation of spin waves in waveguides consisting of magnetic nanostripes has been theoretically considered as a promising way for transmission and processing of information.[14,25] Besides, the exchange of spin waves between spin-torque-transfer nano-oscillators is proved to be an efficient mechanism for their mutual synchronization.[28–30] Therefore, experimental investigations of spin-wave propagation in microscopic waveguides represent a promising task directly related to future technical applications.

Experimental addressing of spin-wave propagation in magnetic nanostructures necessarily demands methods enabling the detection of high-frequency magnetization dynamics with submicrometer spatial resolution. Since such measurements are difficult to realize, until very recently, the studies of spin waves in magnetic microstripes were mainly restricted to the observation of characteristic frequencies and dispersion obtained by means of measurements on large arrays of stripes.[1–4,24] With the development of microfocus Brillouin light scattering (BLS) technique[12] characterized by a spatial resolution down to 250 nm, the direct space-resolved mapping of magnetization dynamics on the submicrometer scale became possible, which allowed the observation of spin-wave radiation patterns[17] and spin-torque-transfer amplification of spin waves.[26] Very recently, the technique was applied for studies of spin-wave excitation and propagation in micrometer-width permalloy stripes.[27] These investigations have shown that the spin-wave quantization results in nontrivial dependencies of the intensity of propagating spin waves on the spatial coordinates. Here, we present a detailed experimental and theoretical analysis of the influence of the spin-wave confinement on propagation of spin waves in permalloy microstripes. We present results of space-resolved measurements of the intensity of propagating spin waves for different widths of the microstripe waveguides, and compare the experimental findings with the results of calculations based on a simple analytical model.

The samples used in the experiments (see Fig. 1) are microstripes patterned by electron-beam lithography from a permalloy film, with the thickness of 20 nm sputter deposited on a glass substrate. The stripes had widths $w=2.1$, 5.1, and 10.1 μm, and a length of 300 μm, and served as long waveguides for spin waves. After the definition of the stripes, they were covered with a transparent 25 nm thick SiO_2 layer for corrosion protection. Afterwards, 300 nm thick Au antennae used for the excitation of spin waves were manufactured. These antennae were patterned in the form of narrow stripes, with the width of 1 μm aligned perpendicularly to the permalloy waveguides. A uniform static magnetic field of $H=300-2000$ Oe was applied in the plane of the magnetic stripes perpendicular to their axis, providing the so-called

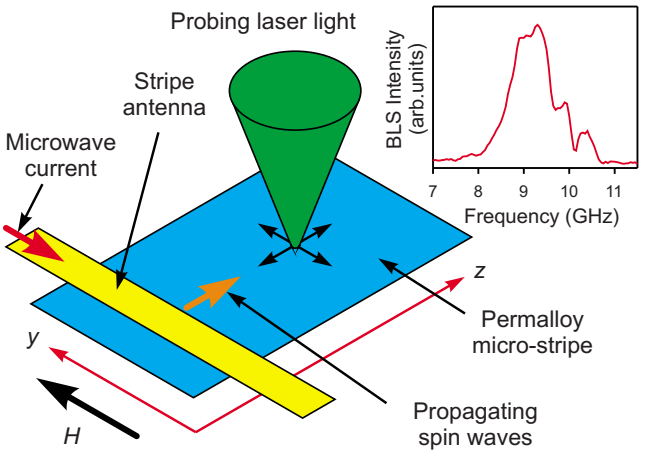

FIG. 1. (Color online) Sketch of the sample used in the experiments. Inset: Spin-wave excitation or transmission characteristic measured for 5.1 μm wide permalloy stripe magnetized by the static field $H=930$ Oe.

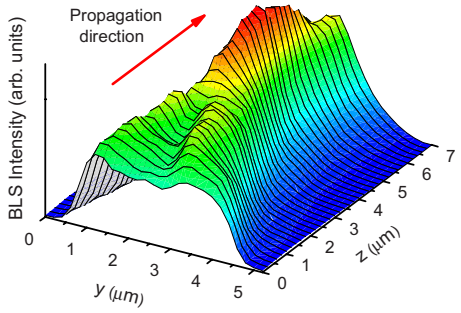

FIG. 2. (Color online) Map of the spin-wave intensity recorded for 5.1 μm wide permalloy stripe with the spatial step size of 0.2 μm. $z=0$ corresponds to the edge of the stripe antenna. The static magnetic field is $H=930$ Oe. The spatial decay is numerically compensated as described in the text.

Damon-Eshbach spin-wave propagation geometry.[31] The spin waves were excited by a monochromatic microwave current through the antennae, with the frequency $f=2-18$ GHz produced by a microwave signal generator. The microwave power was varied in the range from 10 to 200 mW. The spin waves excited in the area of the antenna propagated in the permalloy stripes and were locally detected by BLS spectroscopy.[3] The laser light used as a local probe for the dynamic magnetization was focused onto the surface of the sample (see Fig. 1) and the spectrum of the backscattered light was analyzed with a six-pass tandem Fabry-Pérot interferometer. Since the BLS intensity is proportional to the square of the amplitude of the dynamic magnetization averaged over the precession period, the local spin-wave intensity at the point of the laser focal spot can be directly accessed in this experiment.

The inset in Fig. 1 shows a dependence of the BLS intensity on the excitation frequency measured by positioning the probing laser spot in the middle of a 5.1 μm wide magnetic stripe 3 μm apart from the edge of the antenna for $H=930$ Oe. This dependence can be considered as an excitation or transmission characteristic for spin waves in the magnetic microwaveguide. Its position at the frequency axis is determined by the static magnetic field H, whereas its frequency width is mainly governed by the width of the antenna used for the excitation.[32] In our experimental geometry, an efficient excitation and transmission of spin waves by the permalloy microwaveguide is possible in a frequency window of more than 1 GHz (see inset in Fig. 1), which is wide enough for most of the microwave signal processing applications. In addition, this range can be further extended by reducing the width of the antenna.

By moving the probing laser spot across the sample surface, one can obtain two-dimensional maps of spin-wave intensity characterizing the propagation of spin waves in the microwaveguide. Such a map recorded in a 5.1 μm wide stripe for $H=930$ Oe and the excitation frequency $f=9.2$ GHz is shown in Fig. 2. To simplify the analysis, the mean spatial decay of the spin-wave intensity determined by the high-frequency magnetic dissipation is numerically compensated in this map by multiplying the original data by $\exp(\gamma z)$, where $\gamma=0.5$ μm^{-1} is the mean energy decay parameter obtained from the dependence of the integral of spin-wave intensity across the stripe width on the propagation coordinate z.[27] As seen from the figure, the spin waves do not propagate uniformly along the stripe. Instead, they exhibit a complex dependence of the intensity on the spatial coordinates. Close to the antenna, the transverse spatial profile of the spin-wave beam is rather wide, and has two maxima and a minimum in the middle of the stripe. When traveling away from the antenna, the wave changes its transverse profile and, at a distance $z\approx5$ μm, a pronounced maximum in the middle of the stripe appears. Since the width of the beam decreases, corresponding to a concentration of the spin-wave energy close to the axis of the stripe, the maximum value of the intensity at the stripe axis increases with increasing z. Thus, the propagation process is accompanied by a focusing of the spin-wave beam, with a focal point corresponding to the minimum width of the transverse profile.

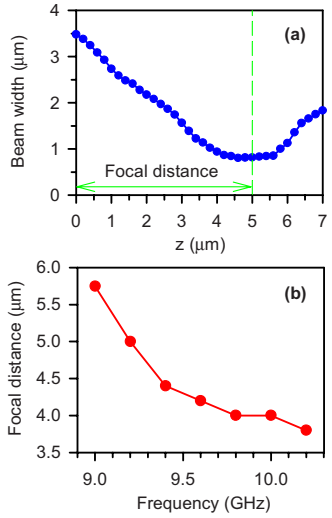

FIG. 3. (Color online) (a) Dependence of the width of the spin-wave beam on the propagation coordinate measured for 5.1 μm wide permalloy stripe at one-half of the maximum intensity. (b) Focal distance as a function of the excitation frequency.

Figure 3(a) shows the dependence of the width of the spin-wave beam as a function of the propagation coordinate for the map shown in Fig. 2. The width was measured at a level of one-half of the maximum spin-wave intensity in corresponding transverse sections. Corroborating the above conclusions, the dependence demonstrates a significant narrowing of the beam from 3.5 μm at $z=0$ to about 0.8 μm at $z=5$ μm. Note that the width of the beam exhibits a plateau around its minimum value. Therefore, it is reasonable to take the coordinate of the middle of this plateau as a focal point. Correspondingly, the distance from the edge of the antenna to the focal point can be treated as the spin-wave focal distance, as marked in Fig. 3(a).

By recording the maps of the spin-wave intensity at different excitation frequencies, we analyzed the spin-wave focal distance for the entire accessible frequency band (see the inset in Fig. 1). The results of these measurements are presented in Fig. 3(b). Note that for the studied propagation geometry, the low-frequency limit of the spin-wave band corresponds to the wave number of the spin waves approaching

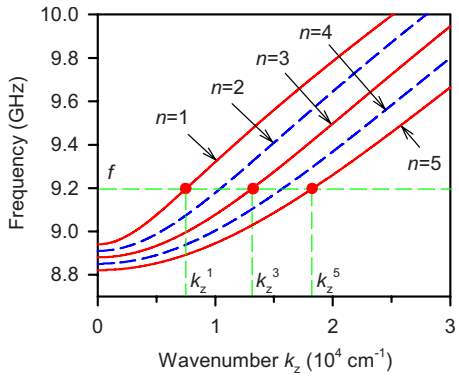

FIG. 4. (Color online) Calculated dispersion spectrum of spin-wave modes in 5.1 μm wide permalloy stripe for $H=930$ Oe. Dispersion curves are shown for the first five modes ($n=1-5$) as indicated. f is the excitation frequency.

zero. Correspondingly, with the increase of the excitation frequency, the wave number increases. As seen from Fig. 3, with increasing excitation frequency (wave number), the focal distance monotonously decreases from 5.8 to 3.8 μm, i.e., by more than 30%.

To understand the experimental findings, we made calculations based on the dipole-exchange theory for spin waves in in-plane magnetized continuous ferromagnetic films developed in Ref. 32. The lateral confinement was taken into account by introducing the quantized component of the wave vector in the direction perpendicular to the stripe axis k_y, whereas the component k_z was assumed to change continuously. The quantization rules were taken from Ref. 6 in the form $k_y=n\pi/w$, where $n=1,2,3\ldots$, is the quantization number. For simplicity, we assumed the boundary conditions of completely pinned dynamic magnetization at the edges of the stripe, corresponding to a vanishing amplitude of the dynamic magnetization at the boundaries. As was shown in Ref. 6, such boundary conditions are a good approximation and their possible slight deviation from the real boundary conditions can be compensated by introducing an effective stripe width w_{eff} to be used as a fitting parameter.

In accordance with the model, the spectrum of spin waves in magnetic stripes consists of a series of dispersion curves corresponding to the spin-wave modes characterized by different quantization numbers n. This dispersion spectrum calculated for the conditions of our experiment is shown in Fig. 4. As seen from the figure, when the exciting dynamic field is applied at a fixed frequency f, several modes are excited simultaneously and copropagate in the ferromagnetic stripe. Since at the same frequency the longitudinal wave numbers k_z are different for different modes, their copropagation should lead to an appearance of a spatially periodic interference pattern. In fact, the appearing spatial structure depends not only on the dispersion characteristics of the spin-wave modes, but also on their excitation characteristics, i.e., on the relative efficiency of excitation of the modes by a source with a given geometry. In our case, the excitation of spin waves is performed with the stripe antenna with a length much smaller than the wavelength of an electromagnetic wave at the used frequencies. Correspondingly, the microwave current and, as a consequence, the exciting magnetic field can be considered as uniform across the width of the magnetic microstripes. It is well known,[33] that such a uniform field can excite the lateral modes with odd quantization numbers n only, and that the amplitude of the dynamic magnetization of the modes decreases with increasing n as $1/n$. For a qualitative reproduction of spatial interference patterns observed in the experiment, it is, therefore, sufficient to consider the copropagation of the first two odd modes with $n=1$ and 3.

In accordance with the assumed quantization rules and the boundary conditions, the spatial distribution of the amplitude of the dynamic magnetization associated with the nth mode can be written as

$$m_n(y,z) \propto \sin\left(\frac{n\pi}{w}y\right)\cos(k_z^n z - \omega t + \varphi_n), \tag{1}$$

where $\omega=2\pi f$ is the cyclic excitation frequency, k_z^n is the longitudinal wave number of the nth spin-wave mode corresponding to this frequency, and φ_n is the excitation phase. Taking $m_n(y,z)^2$ and averaging it over the oscillation period $2\pi/\omega$, we obtain a value proportional to the spin-wave intensity distributions $I_n(y,z)$ corresponding to the first and third modes shown in Figs. 5(a) and 5(b), respectively. In order to calculate their interference pattern, one has to apply the same procedure to the sum $m_1(y,z)+(1/3)m_3(y,z)$, where the coefficient 1/3 takes into account the difference in the excitation efficiency. As a result, we get for the total spin-wave intensity

$$I_\Sigma(y,z) \propto \sin\left(\frac{\pi}{w}y\right)^2 + \frac{1}{9}\sin\left(\frac{3\pi}{w}y\right)^2 + 2\frac{1}{3}\sin\left(\frac{\pi}{w}y\right)\sin\left(\frac{3\pi}{w}y\right)\cos(\Delta k_z z + \Delta\varphi), \tag{2}$$

where $\Delta k_z=k_z^3-k_z^1$ and $\Delta\varphi=\varphi_3-\varphi_1$. As seen from Eq. (2), the spatial interference pattern is periodic along the propagation coordinate with the period $l=2\pi/\Delta k_z$ and the relative phase shift between the modes $\Delta\varphi$ shifts the entire pattern in the z direction. Note that the value Δk_z can be easily calculated within the used approach, whereas for the determination of $\Delta\varphi$, the exact excitation theory is needed, which is out of the scope of this paper. Therefore, in our calculations, we use $\Delta\varphi$ as a fitting parameter.

The interference pattern calculated using Eq. (2) for the conditions of the experiment and $\Delta\varphi=0.1\pi$ is shown in Fig. 5(c). The calculated intensity distribution is qualitatively similar to the measured one shown in Fig. 2. At the position $z=0$, the transverse section of the pattern shows two maxima and a minimum at the axis of the stripe, whereas at the position $z=5$ μm, the section demonstrates only one maximum at the middle line and an increased maximum intensity, which is in accordance with the experimental findings. Therefore, we can conclude that the observed self-focusing effect is mainly governed by the interference of the spin-wave modes with $n=1$ and 3. Further calculations have shown that taking into account higher order modes with n

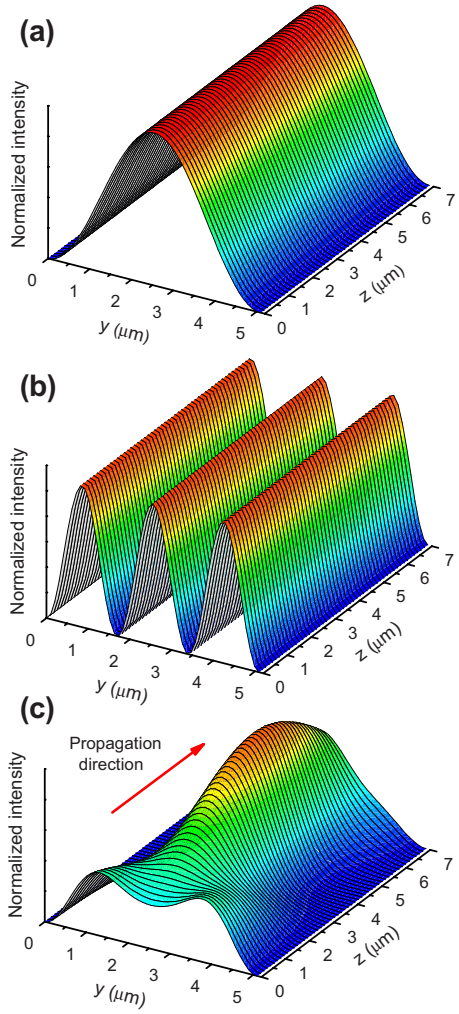

FIG. 5. (Color online) Calculated spatial distributions of the spin-wave intensity for the modes (a) $n=1$ and (b) $n=3$, and (c) their interference pattern. Calculations were performed for the experimental conditions of Fig. 2.

$=5$ and 7 does not change the calculated interference pattern significantly due to their relatively small excitation efficiencies.

Note here that, following Eq. (2), the interference pattern is periodic in the propagation direction, i.e., the spin-wave foci have to appear with the spatial periodicity $l=2\pi/\Delta k_z$. For the 5.1 μm wide stripe, this spatial period is equal to about 11 μm for the excitation frequency of 9.2 GHz. Since this period is comparable to the propagation length of spin waves in thin permalloy films, we could not clearly observe the second focal point in the above experiments. Nevertheless, in narrower stripes, the splitting of the spin-wave spectrum due to the transverse spin-wave quantization appears to be stronger and the value Δk_z becomes larger, leading to a smaller spatial period l. Therefore, the observation of further spin-wave foci should be possible in narrower magnetic stripes.

In order to measure clearly the period of the focusing pattern and compare it with the theoretical one, we studied the spin-wave propagation in 2.1 μm wide permalloy stripes.

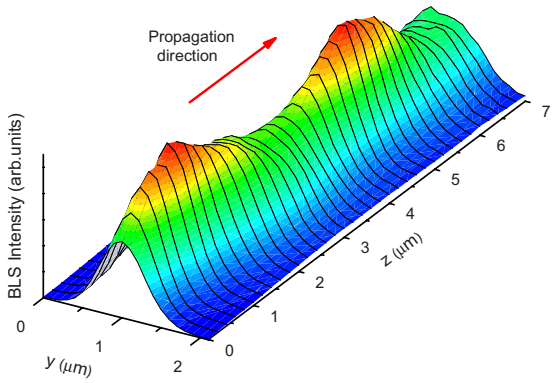

FIG. 6. (Color online) Map of the spin-wave intensity recorded for 2.1 μm wide permalloy stripe with the spatial step sizes of 0.1 and 0.2 μm in the y and z directions, respectively. $z=0$ corresponds to the edge of the stripe antenna. The static magnetic field is $H=930$ Oe. The spatial decay is numerically compensated as described in the text.

An example of the spatial map of the spin-wave intensity obtained for the 2.1 μm wide stripe is shown in Fig. 6. The map was obtained by scanning the area with dimensions of 2.2×7 μm^2 with a spatial step size of 0.1 μm in the y direction and 0.2 μm in the z direction. The map was recorded for the static magnetic field of $H=930$ Oe and the excitation frequency of 9.4 GHz. The homogeneous spatial decay is numerically compensated as described above.

Due to the small width of the stripe, the details of the interference pattern in Fig. 6 are not as well resolved as for the 5.1 μm wide stripe. Nevertheless, one can clearly see in the figure the periodic focusing and defocusing of the spin-wave beam, resulting in a periodic increase of the local spin-wave intensity. Figure 7(a) further characterizes the periodic focusing and defocusing process by showing the dependence of the width of the spin-wave beam on the propagation coordinate. As seen from the figure, the beamwidth exhibits oscillations between 0.5 and 1.1 μm with a well defined spatial period.

In order to obtain the dependence of the spatial period on the excitation frequency, we recorded and analyzed the maps of spin-wave intensity within the entire spin-wave excitation band of 8.8–10 GHz. Note that the dispersion curves of spin waves in 2.1 μm wide stripes at a given value of the external magnetic field are shifted downward by about 0.2 GHz in comparison with those for 5.1 μm wide stripes due to the stronger demagnetization field. The results of these measurements are presented in Fig. 7(b) by points. Similar to the spin-wave focal distance obtained for wider stripe, the full spatial period of the focusing pattern decreases with increasing spin-wave frequency (wave number). The obtained spatial period can be directly compared with that calculated within the used model without the need to know the excitation phase shift $\Delta\varphi$. The results of calculations obtained without using any fitting parameters are presented in Fig. 7(b) by the dashed line. As seen from the figure, the calculated period is slightly larger than the experimentally measured one. The reason for this slight disagreement can be the difference of the used boundary conditions of completely

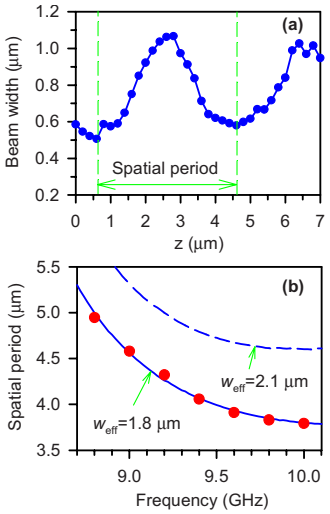

FIG. 7. (Color online) (a) Dependence of the width of the spin-wave beam on the propagation coordinate measured for 2.1 μm wide permalloy stripe at one-half of the maximum intensity. (b) Dependence of the spatial period of the interference pattern on the excitation frequency: points, experimental data; lines, results of calculations for different effective widths of the stripe as indicated.

pinned magnetization from the real ones and by the nonuniformity of the internal static magnetic field inside the stripe due to demagnetization effects. As suggested in Ref. 6, these deviations can be taken into account by introducing an effective width of the stripe w_{eff}, which differs from the nominal width w. Using the width as a fitting parameter, we were able to obtain a perfect agreement between the experimental and theoretical results for $w_{\mathrm{eff}}=1.8$ μm [see solid line in Fig. 7(b)]. Note that the obtained effective width is slightly smaller than w, which is typical for transversally magnetized stripes and is mainly governed by the nonuniformity of the internal static magnetic field.[10]

In conclusion, we have studied experimentally and theoretically the propagation of spin waves in transversally magnetized microscopic permalloy stripes. We show that several spin-wave modes quantized in the direction perpendicular to the stripe axis are simultaneously excited in the stripes. The copropagation of these modes leads to a spatial interference pattern demonstrating periodic focusing and defocusing of the spin waves, resulting in a periodic local increase of the spin-wave intensity in the middle line of the stripe. This process is well described within a model taking into account the first two odd spin-wave modes. These findings are important for the design and optimization of microscopic waveguides to be used for, e.g., transmission of spin waves in magnetic circuits for microelectronics.

This work was supported in part by the priority program SPP1133 "Ultrafast magnetization processes" of the Deutsche Forschungsgemeinschaft.

*demidov@uni-muenster.de

[1] C. Mathieu, J. Jorzick, A. Frank, S. O. Demokritov, A. N. Slavin, B. Hillebrands, B. Bartenlian, C. Chappert, D. Decanini, F. Rousseaux, and E. Cambril, Phys. Rev. Lett. **81**, 3968 (1998).

[2] J. Jorzick, S. O. Demokritov, C. Mathieu, B. Hillebrands, B. Bartenlian, C. Chappert, F. Rousseaux, and A. N. Slavin, Phys. Rev. B **60**, 15194 (1999).

[3] S. O. Demokritov, B. Hillebrands, and A. N. Slavin, Phys. Rep. **348**, 441 (2001).

[4] Y. Roussigne, S. M. Cherif, C. Dugautier, and P. Moch, Phys. Rev. B **63**, 134429 (2001).

[5] J. Jorzick, S. O. Demokritov, B. Hillebrands, M. Bailleul, C. Fermon, K. Y. Guslienko, A. N. Slavin, D. V. Berkov, and N. L. Gorn, Phys. Rev. Lett. **88**, 047204 (2002).

[6] K. Yu. Guslienko, S. O. Demokritov, B. Hillebrands, and A. N. Slavin, Phys. Rev. B **66**, 132402 (2002).

[7] J. P. Park, P. Eames, D. M. Engebretson, J. Berezovsky, and P. A. Crowell, Phys. Rev. B **67**, 020403(R) (2003).

[8] T. M. Crawford, M. Covington, and G. J. Parker, Phys. Rev. B **67**, 024411 (2003).

[9] G. Gubbiotti, G. Carlotti, T. Okuno, T. Shinjo, F. Nizzoli, and R. Zivieri, Phys. Rev. B **68**, 184409 (2003).

[10] K. Y. Guslienko, R. W. Chantrell, and A. N. Slavin, Phys. Rev. B **68**, 024422 (2003).

[11] M. Grimsditch, G. K. Leaf, H. G. Kaper, D. A. Karpeev, and R. E. Camley, Phys. Rev. B **69**, 174428 (2004).

[12] V. E. Demidov, S. O. Demokritov, B. Hillebrands, M. Laufenberg, and P. P. Freitas, Appl. Phys. Lett. **85**, 2866 (2004).

[13] M. Buess, R. Höllinger, T. Haug, K. Perzlmaier, U. Krey, D. Pescia, M. R. Scheinfein, D. Weiss, and C. H. Back, Phys. Rev. Lett. **93**, 077207 (2004).

[14] R. Hertel, W. Wulfhekel, and J. Kirschner, Phys. Rev. Lett. **93**, 257202 (2004).

[15] B. A. Ivanov and C. E. Zaspel, Phys. Rev. Lett. **94**, 027205 (2005).

[16] K. Perzlmaier, M. Buess, C. H. Back, V. E. Demidov, B. Hillebrands, and S. O. Demokritov, Phys. Rev. Lett. **94**, 057202 (2005).

[17] V. E. Demidov, S. O. Demokritov, B. Hillebrands, M. Laufenberg, and P. P. Freitas, J. Appl. Phys. **97**, 10A717 (2005).

[18] J. Raabe, C. Quitmann, C. H. Back, F. Nolting, S. Johnson, and C. Buehler, Phys. Rev. Lett. **94**, 217204 (2005).

[19] J. P. Park and P. A. Crowell, Phys. Rev. Lett. **95**, 167201 (2005).

[20] C. Bayer, J. Jorzick, B. Hillebrands, S. O. Demokritov, R. Kouba, R. Bozinoski, A. N. Slavin, K. Y. Guslienko, D. V. Berkov, N. L. Gorn, and M. P. Kostylev, Phys. Rev. B **72**, 064427 (2005).

[21] J. Podbielski, F. Giesen, and D. Grundler, Phys. Rev. Lett. **96**, 167207 (2006).

[22] M. Bailleul, R. Höllinger, and C. Fermon, Phys. Rev. B **73**, 104424 (2006).

[23] I. Neudecker, M. Kläui, K. Perzlmaier, D. Backes, L. J. Heyderman, C. A. F. Vaz, J. A. C. Bland, U. Rüdiger, and C. H. Back, Phys. Rev. Lett. **96**, 057207 (2006).

[24] M. P. Kostylev, G. Gubbiotti, J.-G. Hu, G. Carlotti, T. Ono, and

R. L. Stamps, Phys. Rev. B **76**, 054422 (2007).
[25] S. Choi, K.-S. Lee, K. Yu. Guslienko, and S.-K. Kim, Phys. Rev. Lett. **98**, 087205 (2007).
[26] V. E. Demidov, S. O. Demokritov, G. Reiss, and K. Rott, Appl. Phys. Lett. **90**, 172508 (2007).
[27] V. E. Demidov, S. O. Demokritov, K. Rott, P. Krzysteczko, and G. Reiss, Appl. Phys. Lett. **91**, 252504 (2007).
[28] S. Kaka, M. R. Pufall, W. H. Rippard, T. J. Silva, S. E. Russek, and J. A. Katine, Nature (London) **437**, 389 (2005).
[29] F. B. Mancoff, N. D. Rizzo, B. N. Engel, and S. Tehrani, Nature (London) **437**, 393 (2005).
[30] M. R. Pufall, W. H. Rippard, S. E. Russek, S. Kaka, and J. A. Katine, Phys. Rev. Lett. **97**, 087206 (2006).
[31] R. W. Damon and J. R. Eshbach, J. Phys. Chem. Solids **19**, 308 (1961).
[32] B. A. Kalinikos, IEE Proc., Part H: Microwaves, Opt. Antennas **127**, 4 (1980).
[33] C. Kittel, Phys. Rev. **110**, 1295 (1958).